Damage Identification in Thin Steel Beams Containing a Horizontal Crack Using the Artificial Neural Networks

Amirhossein Heshmati[1], Morteza Saadatmorad[1], Ramazan-Ali Jafari Talookolaei[1(✉)], Paolo S. Valvo[2], and Samir Khatir[3]

[1] School of Mechanical Engineering, Babol Noshirvani University of Technology, Babol, Mazandaran, Iran
`ramazanali@gmail.com, ra.jafari@nit.ac.ir`
[2] Department of Civil and Industrial Engineering, University of Pisa, Pisa, Italy
[3] Ho Chi Minh City Open University, Ho Chi Minh City, Vietnam

Abstract. This investigation presents damage identification in thin steel beams containing a horizontal crack using artificial neural networks. In this way, finite element modeling of the cracked beam is developed to generate natural frequencies corresponding to various horizontal cracks scenarios. Then, the artificial neural network is used to create a predictor model for localizing horizontal cracks in steel beams. Results of the current paper show that The proposed technique is an effective method for detecting horizontal crack damage in steel beams. The regression index obtained in this study is equal to 0.979.

Keywords: Structural health monitoring · Damage identification · Artificial neural networks · Steel beams · Horizontal cracks

1 Introduction

Structural analysis and structural health monitoring are two essential issues in structural engineering from nano size to macro size [1–10]. The objective of structural health monitoring is to prevent the failure of structures [11–14]. As a result, structural health monitoring prevents additional costs for repairing and reconstruction of damaged structures [15–17]. In this regard, vibration-based analysis of damaged structures plays an essential role in structural health monitoring [18–22]. Generally, there are two main types of analysis of damaged structures: Forward analysis and inverse analysis [23–28].

The forward analysis deals with modeling damages to provide modal characteristics of structures such as mode shapes and their corresponding natural frequencies [29–32]. Also, the forward analysis may use to obtain dynamic responses of the damaged structures [33–36]. In this field, much research has been conducted.

In reverse analysis, on the other hand, the goal is to obtain the position or extent of the damage by having the vibrational properties of the system. So far, much research has been done in this area. Some of these approaches are based on optimization, a part of them are based on the mode shapes, the others are based on machine learning

algorithms. In this research, one of the machine learning algorithms called the artificial neural network algorithm is used to detect horizontal cracks in steel beams, including a vertical crack. In this way, first, the modeling of finite components of horizontal cracks in steel beams is described in the next section. Then the artificial neural network is introduced, the technique proposed in this paper, and then numerical examples and results are presented, and finally, conclusions are presented.

2 Basic Mathematical Formulations

2.1 Geometry

In order to investigate the damage identification problem, a thin isotropic beam of length L with a rectangular cross-sectional area A, width b, and thickness h is modeled in the same procedure as [37]. As shown in Fig. 1-b, the damaged beam is modeled by the combination of four intact sub-beams, which is separated by a through-the-width horizontal crack of length L_2 which is located at the midplane and a distance L_1 from the left end of the beam. In this manner, each sub-beam has a length and thickness of $L_i \times h_i (i = 1 - 4)$ where i represents the number of sub-beams, $h_1 = h_4 = h$, $L_2 = L_3$, and $L_4 = L - L_1 - L_2$.
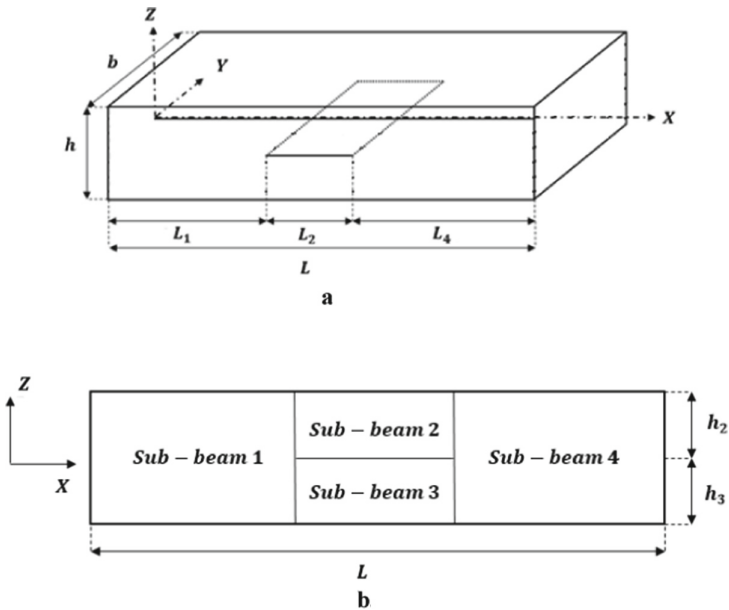

Fig. 1. a. The geometry of isotropic beam, b. Representation of beam into four sub-beams.

2.2 Finite Element Modeling

To study the vibration analysis of the presented beam, in this paper, the Euler-Bernoulli beam theory is adopted to establish vibration equations. Therefore, a higher-order beam

element as demonstrated in Fig. 2 with three nodes and six degrees of freedom, including vertical displacement w and slope w' is introduced.
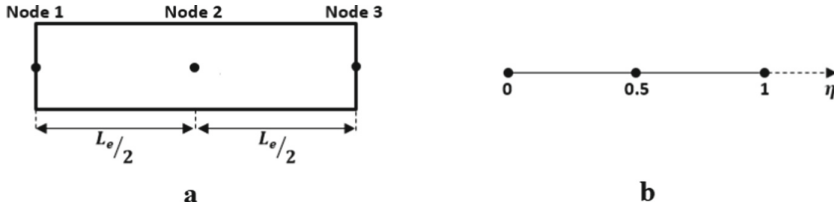

Fig. 2. (a) Higher-order beam element. (b) intrinsic coordinate of the element

The displacement field equation for the higher-order beam element can be interpolated via the Hermite interpolation function and in terms of the intrinsic coordinate as:

$$w = \sum_{i=1}^{3}\left[w_{2i-1}(\eta)w_i + \Lambda_{2i}(\eta)w_i'\right] = [\Lambda]\{d\} \tag{1}$$

where η is the intrinsic coordinate, i.e. $\eta = \frac{x}{L_e}$ and L_e is the length of the respective element. As well, $\{d\}$ indicates the vector of DOFs and $\Lambda_i(\eta)$ are the shape functions associated with i th degrees of freedom which are given as:

$$\Lambda_1(\eta) = 1 - 23\eta^2 + 66\eta^3 - 68\eta^4 + 24\eta^5$$

$$\Lambda_2(\eta) = L_e(\eta - 6\eta^2 + 13\eta^3 - 12\eta^4 + 4\eta^5)$$

$$\Lambda_3(\eta) = 16\eta^2 - 32\eta^3 + 16\eta^4$$

$$\Lambda_4(\eta) = L_e(-8\eta^2 + 32\eta^3 - 40\eta^4 + 16\eta^5)$$

$$\Lambda_5(\eta) = 7\eta^2 - 34\eta^3 + 52\eta^4 - 24\eta^5$$

$$\Lambda_6(\eta) = L_e\left(-\eta^2 + 5\eta^3 - 8\eta^4 + 4\eta^5\right) \tag{2}$$

$$\{d\} = \{w_1 \; w_1' \; w_2 \; w_2' \; w_2 \; w_3'\} \tag{3}$$

The energy approach is utilized to obtain the element stiffness and mass matrices, which is not described in detail here [38, 39]. Hence, the potential and kinetic energy of an element can be stated in terms of displacement vector as follows [40]:

$$U_e = \frac{1}{2}\{d\}^T[K_e]\{d\} \tag{4}$$

$$T_e = \frac{1}{2}\{\dot{d}\}^T [M_e]\{\dot{d}\} \tag{5}$$

Thus, the element stiffness matrix can be obtained as:

$$[K_e] = \int_0^1 (EI)_e [\Lambda_{,xx}]^T [\Lambda_{,xx}] L_e d\eta \tag{6}$$

Likewise, the element mass matrix can be expressed as follows:

$$[M_e] = \int_0^1 m_e [\Lambda]^T [\Lambda] L_e d\eta \tag{7}$$

In which, m_e and $(EI)_e$ are the density and flexural stiffness of the typical element, respectively.

Equations (6) and (7) give the element stiffness and mass matrices of each sub-beams. To obtain the total corresponding matrices $[K]$ and $[M]$, the stiffness and mass matrices are assembled. To do this, the displacement continuity conditions have been established at the junction of sub-beams (1-2-3) and (2-3-4). Regarding Fig. 3, the deflection and slope of the connecting nodes at the tips of the crack are equal. Therefore, the corresponding entries of the stiffness and mass matrices of connected sub-beams are superposed to constitute the whole beam's total stiffness and mass matrices.
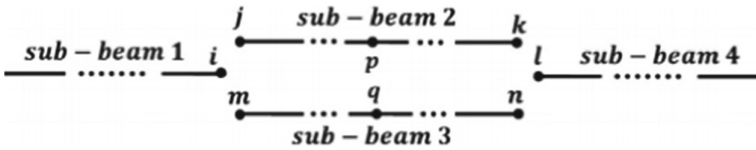

Fig. 3. Delamination boundaries

2.3 Solution Method

The free vibrations equation of motion for the entire structure is acquired as follows:

$$[M]\{\ddot{\Delta}\} + [K]\{\Delta\} = \{0\} \tag{8}$$

where $[\Delta]$ Indicates the nodal DOFs of the whole model. Considering a general solution of $\{\Delta\} = \{\Delta_0\}e^{\hat{i}\omega t}$ for Eq. (8), and assuming $\lambda = \omega^2$ yields eigenvalue problem as:

$$([K] - \lambda[M])\{\Delta_0\} = \{0\} \tag{9}$$

Which gives natural frequency ω and corresponding mode shapes of the system $\{\Delta\}$.

2.4 Artificial Neural Network

This study uses a feed-forward ANN to localize damage levels in beams with horizontal cracks. Figure 4 indicates that our MLP contains the input, hidden, and output layers. Nodes in hidden and output layers utilize a non-linear function.

The weighted sum of input data is calculated as following [41]:

$$input_k = \sum_{i,k=1}^{n,m} b_k + w_{ik} * x_i; \; k = (1:m); \; i = (1:n) \tag{10}$$

where w_{ik} show weight between the ith neurons and the kth neurons, b_k indicates the bias ratio of hidden layers and inputs; x_i show the output in i^{th} neurons in the input layer; m and n are the number of the neurons in hidden layer and input layer, respectively. Furthermore, $input_k$ are the input of kth neurons in the hidden layer.
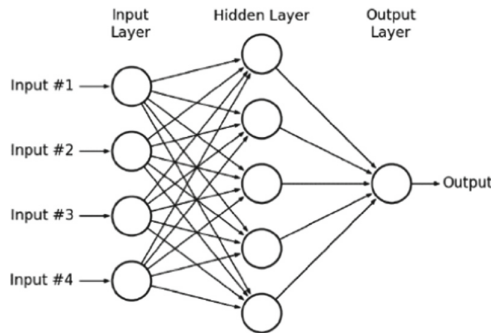

Fig. 4. Architecture of an MLP [41]

In this article, after calculating the $input_k$ of a neuron on a layer, the nonlinear function is applied through the following relation to compute the output for the jth neuron [41]:

$$ouput_j = \left(\frac{2}{1 + \frac{1}{e^{2input_q}}} \right) - 1 \tag{11}$$

The function is called the Tan-Sigmoid transfer function. The diagram of such a function is shown in Fig. 5.
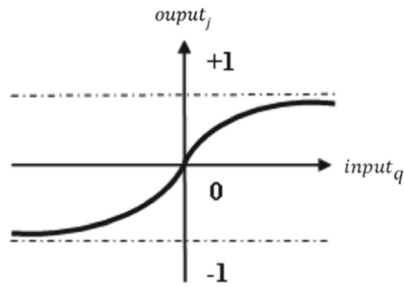
Fig. 5. Tan-Sigmoid activation function [41]

Note that, in Eq. (11), $input_q$ is input of qth neuron in the output layer, and $ouput_j$ denotes j^{th} neuron related to the output layer.

3 Proposed Approach

The current study uses a machine learning-based approach to damage detection in steel beam structures with a horizontal crack. Figure 6 shows the flowchart of the proposed technique used in the present study. As seen, the finite element method performs problem modeling using the equivalence technique of a damaged beam with a horizontal crack approximated with four intact beams. A database is then created to perform the interpolation by the Artificial Neural Network.
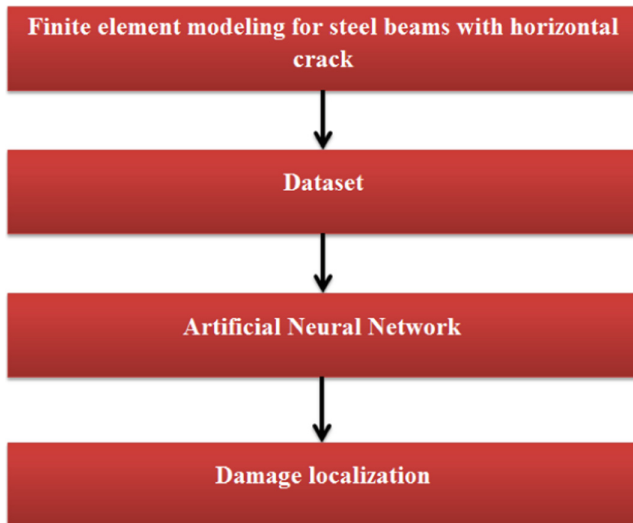

Fig. 6. Flowchart of the proposed technique used in the present study

In this way, the artificial neural network inputs are the first five natural frequencies. The artificial neural network output is the location of the horizontal crack of the desired size in the considered steel beam. In the next section, results are presented.

4   Results and Discussion

The results of this study is presented in this section. The characterisitcs of the considered beam are presented in Table 1. Three hundred samples of the first five natural frequencies and their corresponding crack positions are used as databases to evaluate the method's performance presented in this paper.

Table 1. The characterisitcs of the considered beam

Characterisitcs	Values
Length	100 (cm)
Thickness	1 (cm)
Width	1 (cm)
Young modulus	200 (Gpa)
Density	7800 (Kg/m^3)
Crack length	0.3 (cm)
Number of element	500

The distribution of the Artificial Neural Network outputs (horizontal crack positions) is shown in Fig. 7. As can be seen, the distribution of artificial neural network outputs used in this research is uniform. Also, the horizontal crack length of the beam in this research is 0.3 cm, which is small enough to detect damage.
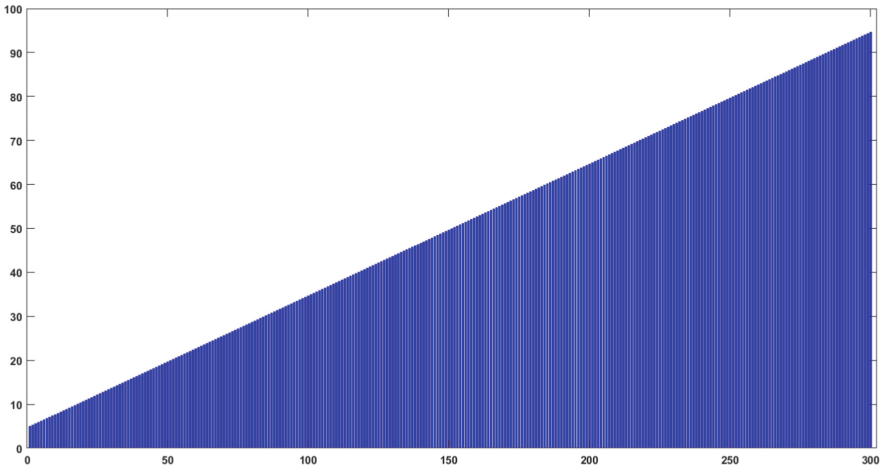
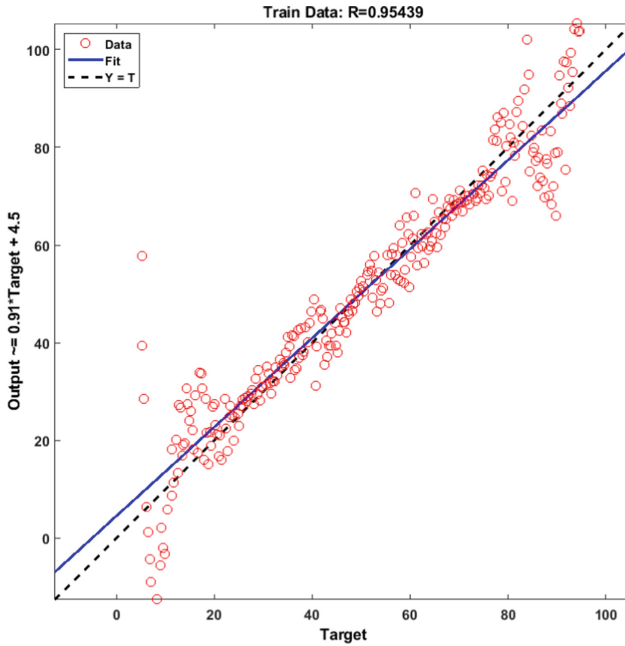**Fig. 7.** The distribution of artificial neural network outputs

Fig. 8. Result of training process of ANN

Result of training process is shown in Fig. 8. Also, Result of test process is shown in Fig. 9.

Figures 8 and 9 show that the regression indices for training and testing processes are 0.954 and 0.979, respectively, demonstrating our predicting model's good approximation and efficiencies. Figure 10 shows the accuracy of the model created in this research.
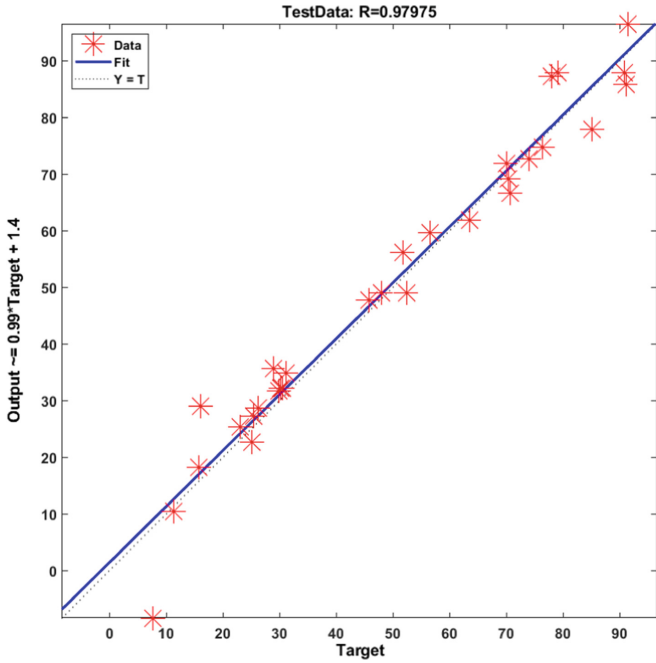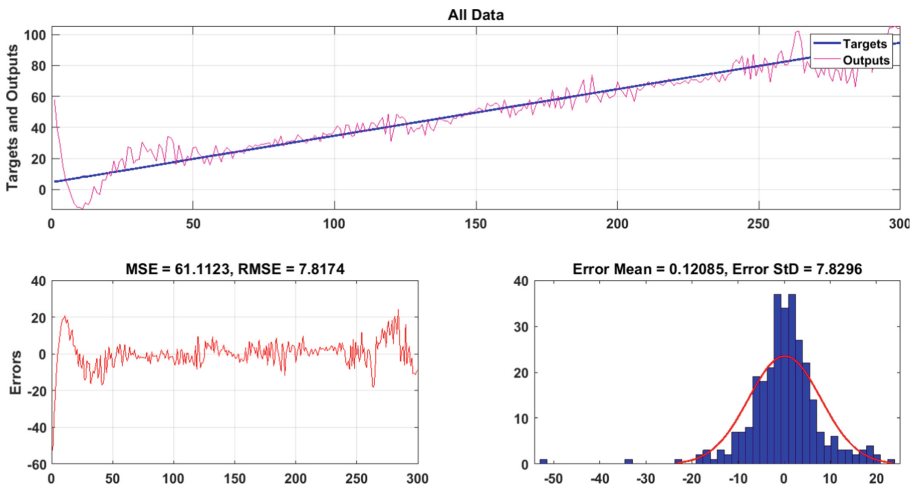
Fig. 9. Result of training process of ANN

Fig. 10. The accuracy of the model created in this research

Figure 11 presents the accuracy of the predictive ANN model for seventeen damage scenarios. As can be seen, ANN identifies the approximate location of the damages with sufficient certainty for the considered damages.
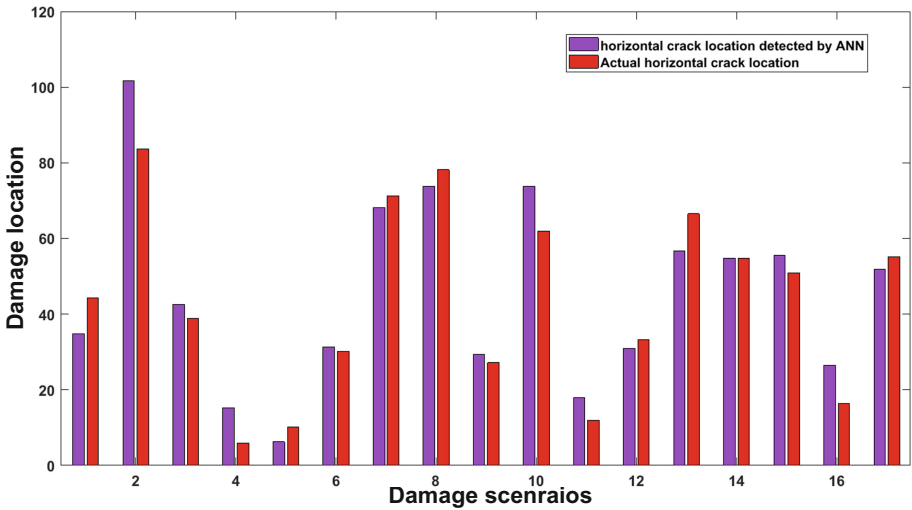
Fig. 11. Seventeen damage scenarios for evaluating the accuracy of the predictive ANN model

Also, to imagine the quantified numerical differences between the actual location of the crack and the location of crack detected by ANN, Table 2 is presented.

Table 2. The quantified numerical differences between the actual location of the crack and the location of crack detected by ANN

No.	Actual location of crack (cm)	Location of crack detected by ANN (cm)
1	34.8745477050543	44.3000000000000
2	54.8354852050543	54.8000000000000
3	42.5893914550543	38.9000000000000
4	68.1792352050543	71.3000000000000
5	6.21048520505428	10.1000000000000
6	31.3589227050543	30.2000000000000
7	68.1792352050543	71.3000000000000
8	73.7651727050543	78.2000000000000

As listed in Table 2, the location of cracks detected by ANN is well compatible with the actual location of cracks.

5   Conclusions

Structural health monitoring is one of the most critical efforts to prevent the failure of the structures before it occurs. Various methods have been proposed to monitor the

structure's health, many of which are considered non-destructive tests. One of the most popular non-destructive tests is vibration-based non-destructive tests. These tests are also known as vibration-based damage detection techniques. In this research, the detection of damage to steel beams with a horizontal crack is investigated using artificial neural networks. In this way, first, a beam is equated with a horizontal crack with four intact beams. In this way, the finite element method is used. After modeling, they are using the finite element method, databases consisting of the first five natural frequencies and the position of the horizontal crack in the steel beam are created and fed to the artificial neural network. The results of this study show that the neural network created in this paper can predict the crack position with acceptable accuracy by having the first five natural frequencies.

References

1. Khatir, S., Belaidi, I., Khatir, T., Hamrani, A., Zhou, Y.L., Wahab, M.A.: Multiple damage detection in composite beams using Particle Swarm Optimization and Genetic Algorithm. Mechanics **23**(4), 514–521 (2017), 4, 487–509, 2011
2. Mashhadzadeh, A.H., Fathalian, M., Ahangari, M.G., Shahavi, M.H.: DFT study of Ni, Cu, Cd and Ag heavy metal atom adsorption onto the surface of the zinc-oxide nanotube and zinc-oxide graphene-like structure. Mater. Chem. Phys. **220**, 366–373 (2018)
3. Hassanpour, M., et al.: Ionic liquid-mediated synthesis of metal nanostructures: Potential application in cancer diagnosis and therapy. J. Ionic Liquids **2**, 100033 (2022)
4. Mofidian, R., Barati, A., Jahanshahi, M., Shahavi, M.H.: Optimization on thermal treatment synthesis of lactoferrin nanoparticles via Taguchi design method. SN Appl. Sci. **1**(11), 1–9 (2019). https://doi.org/10.1007/s42452-019-1353-z
5. Kazemeini, H., Azizian, A., Shahavi, M.H.: Effect of chitosan nano-gel/emulsion containing bunium persicum essential oil and nisin as an edible biodegradable coating on escherichia coli o157: H7 in rainbow trout fillet. J. Water Environ. Nanotechnol. **4**(4), 343–349 (2019)
6. Jafari, B., Khatamnejad, H., Shahavi, M.H., Domeyri Ganji, D.: Simulation of dual fuel combustion of direct injection engine with variable natural gas premixed ratio. Int. J. Eng. **32**(9), 1327–1336 (2019)
7. Sun, Z., Nagayama, T., Nishio, M., Fujino, Y.: Investigation on a curvature-based damage detection method using displacement under moving vehicle. Struct. Control. Health Monit. **25**(1), e2044 (2018)
8. Fathi, A., Limongelli, M.P.: Statistical vibration-based damage localization for the S101 bridge. Flyover Reibersdorf, Austria. Struct. Infrastructure Eng. **17**(6), 857–871 (2021). Guo, J., Hu, C. J., Zhu, M. J., & Ni, Y. Q. (2021)
9. Guo, J., Hu, C.-J., Zhu, M.-J., Ni, Y.-Q.: Monitoring-based evaluation of dynamic characteristics of a long span suspension bridge under typhoons. J. Civ. Struct. Heal. Monit. **11**(2), 397–410 (2021). https://doi.org/10.1007/s13349-020-00458-5
10. Khatir, S., Tiachacht, S., Benaissa, B., Le Thanh, C., Capozucca, R., Abdel Wahab, M.: Damage Identification in Frame Structure Based on Inverse Analysis. In: Wahab, M.A. (ED.) SDMA 2021, pp. 197–211. Springer, Singapore (2022). DOI: https://doi.org/10.1007/978-981-16-7216-3_15
11. Saadatmorad, M., Jafari-Talookolaei, R.A., Pashaei, M.H., Khatir, S.: Damage detection on rectangular laminated composite plates using wavelet based convolutional neural network technique. Compos. Struct. **278**, 114656 (2021)
12. Limongelli, M.P., et al.: Vibration Response-Based Damage Detection. Structural Health Monitoring Damage Detection Systems for Aerospace, 133 (2021)

13. Saadatmorad, M., Jafari-Talookolaei, R.A., Pashaei, M.H., Khatir, S., Abdel Wahab, M.: Adaptive network-based fuzzy inference for damage detection in rectangular laminated composite plates using vibrational data. In: Abdel Wahab, M. (ed.) Proceedings of the 2nd International Conference on Structural Damage Modelling and Assessment, pp. 179–196. Springer, Singapore (2022). Doi: https://doi.org/10.1007/978-981-16-7216-3_14

14. Saadatmorad, M., Jafari-Talookolaei, R.A., Pashaei, M.H., Khatir, S., Abdel Wahab, M.: Application of multilayer perceptron neural network for damage detection in rectangular laminated composite plates based on vibrational analysis. In: Abdel Wahab, M. (ed.) Proceedings of the 2nd International Conference on Structural Damage Modelling and Assessment, pp. 163–178. Springer, Singapore (2022). Doi: https://doi.org/10.1007/978-981-16-7216-3_13

15. Pisani, M.A., Limongelli, M.P., Giordano, P.F., Palermo, M.: On the effectiveness of vibration-based monitoring for integrity management of prestressed structures. Infrastructures **6**(12), 171 (2021)

16. Khatir, S., Dekemele, K., Loccufier, M., Khatir, T., Wahab, M.A.: Crack identification method in beam-like structures using changes in experimentally measured frequencies and Particle Swarm Optimization. Comptes Rendus Mécanique **346**(2), 110–120 (2018)

17. Behtani, A., Tiachacht, S., Khatir, T., Khatir, S., Wahab, M.A., Benaissa, B.: Residual Force Method for damage identification in a laminated composite plate with different boundary conditions. Frattura ed Integrità Strutturale **16**(59), 35–48 (2022)

18. Tiachacht, S., Bouazzouni, A., Khatir, S., Wahab, M.A., Behtani, A., Capozucca, R.: Damage assessment in structures using combination of a modified Cornwell indicator and genetic algorithm. Eng. Struct. **177**, 421–430 (2018)

19. Saadatmorad, M., Siavashi, M., Jafari-Talookolaei, R.A., Pashaei, M.H., Khatir, S., Thanh, C.L.: Multilayer perceptron neural network for damage identification based on dynamic analysis. In: Bui, T.Q., Cuong, L.T., Khat, S. (ed.) Structural Health Monitoring and Engineering Structures, pp. 29–48. Springer, Singapore (2021). Doi: https://doi.org/10.1007/978-981-16-0945-9_3

20. Khatir, S., Tiachacht, S., Le Thanh, C., Ghandourah, E., Mirjalili, S., Wahab, M.A.: An improved artificial neural network using arithmetic optimization algorithm for damage assessment in FGM composite plates. Compos. Struct. **273**, 114287 (2021)

21. Benaissa, B., Hocine, N.A., Khatir, S., Riahi, M.K., Mirjalili, S.: YUKI Algorithm and POD-RBF for Elastostatic and dynamic crack identification. J. Comput. Sci. **55**, 101451 (2021)

22. Saadatmorad, M., Siavashi, M., Jafari-Talookolaei, R.A., Pashaei, M.H., Khatir, S., Thanh, C.L.: Genetic and particle swarm optimization algorithms for damage detection of beam-like structures using residual force method. In: Structural Health Monitoring and Engineering Structures, pp. 143-157. Springer, Singapore (2021)

23. Yang, Y., Liu, H., Mosalam, K.M., Huang, S.: An improved direct stiffness calculation method for damage detection of beam structures. Struct. Control. Health Monit. **20**(5), 835–851 (2013)

24. Park, H.S., Oh, B.K.: Damage detection of building structures under ambient excitation through the analysis of the relationship between the modal participation ratio and story stiffness. J. Sound Vib. **418**, 122–143 (2018)

25. Wahab, M.A., De Roeck, G.: Damage detection in bridges using modal curvatures: application to a real damage scenario. J. Sound Vibration, **226**(2), 217–235 (1999)

26. Yazdanpanah, O., Seyedpoor, S.M.: A new damage detection indicator for beams based on mode shape data. Struct. Eng. Mech. **53**(4), 725–744 (2015)

27. Dahak, M., Touat, N., Kharoubi, M.: Damage detection in beam through change in measured frequency and undamaged curvature mode shape. Inverse Probl. Sci. Eng. **27**(1), 89–114 (2019)

28. Ratcliffe, C.P.: Damage detection using a modified Laplacian operator on mode shape data. J. Sound Vib. **204**(3), 505–517 (1997)

29. Jafari-Talookolaei, R.A., Abedi, M., Hajianmaleki, M.: Vibration characteristics of generally laminated composite curved beams with single through-the-width delamination. Composite Struct. **138**, 172–183 (2016)
30. Jafari-Talookolaei, R. A., & Abedi, M. (2014). Analytical solution for the free vibration analysis of delaminated Timoshenko beams. The Scientific World Journal (2014)
31. OmidDezyani, S., Jafari-Talookolaei, R. A., Abedi, M., Afrasiab, H.: Vibration analysis of a microplate in contact with a fluid based on the modified couple stress theory. Modares Mech. Eng. **17**(2), 47–57 (2017)
32. Jafari-Talookolaei, R.A., Kargarnovin, M.H., Ahmadian, M.T., Abedi, M.: An investigation on the nonlinear free vibration analysis of beams with simply supported boundary conditions using four engineering theories. J. Appl. Math. **2011**, 1–17 (2011)
33. Ramian, A., Jafari-Talookolaei, R.A., Valvo, P.S., Abedi, M.: Free vibration analysis of sandwich plates with compressible core in contact with fluid. Thin-Walled Struct. **157**, 107088 (2020)
34. Jafari-Talookolaei, R.A., Abedi, M., Kargarnovin, M.H., Ahmadian, M.T.: Dynamic analysis of generally laminated composite beam with a delamination based on a higher-order shear deformable theory. J. Compos. Mater. **49**(2), 141–162 (2015)
35. Jafari-Talookolaei, R.A., Abedi, M., Kargarnovin, M.H., Ahmadian, M.T.: Dynamics of a generally layered composite beam with single delamination based on the shear deformation theory. Sci. Eng. Compos. Mater. **22**(1), 57–70 (2015)
36. Jafari-Talookolaei, R.A., Kargarnovin, M. H., Ahmadian, M. T., & Abedi, M. (2011). Analytical expressions for frequency and buckling of large amplitude vibration of multilayered composite beams. Advances in Acoustics and Vibration, 2011
37. Jafari-Talookolaei, R.A., Kargarnovin, M.H., Ahmadian, M.T.: Dynamic response of a delaminated composite beam with general lay-ups based on the first-order shear deformation theory. Compos. Part B: Eng. **55**, 65–78 (2013)
38. Jafari-Talookolaei, R.A., Abedi, M., Attar, M.: In-plane and out-of-plane vibration modes of laminated composite beams with arbitrary lay-ups. Aeros. Sci. Technol. **66**, 366–379 (2017)
39. Kargarnovin, M.H., Ahmadian, M.T., Jafari-Talookolaei, R.A., Abedi, M.: Semi-analytical solution for the free vibration analysis of generally laminated composite Timoshenko beams with single delamination. Compos. Part B: Eng. **45**(1), 587–600 (2013)
40. Jafari-Talookolaei, R.A., Kargarnovin, M.H., Ahmadian, M.T.: Free vibration analysis of cross-ply layered composite beams with finite length on elastic foundation. Int. J. Comput. Methods **5**(01), 21–36 (2008)
41. Zainal-Mokhtar, K., Mohamad-Saleh, J.: An oil fraction neural sensor developed using electrical capacitance tomography sensor data. Sensors **13**(9), 11385–11406 (2013)